LHCD and ICRF heating experiments in H-mode plasmas on EAST

X. J. Zhang, Y. P. Zhao, B. N. Wan, B. J. Ding, G. S. Xu, X. Z. Gong, J. G. Li, Y. Lin, G. Taylor, J. M. Noterdaeme, F. Braun, S. Wukitch, R. Magne, X. Litaudon, R. Kumazawa, H. Kasahara, and EAST Team

Citation: AIP Conference Proceedings **1580**, 49 (2014); doi: 10.1063/1.4864501
View online: http://dx.doi.org/10.1063/1.4864501
View Table of Contents: http://scitation.aip.org/content/aip/proceeding/aipcp/1580?ver=pdfcov
Published by the AIP Publishing

LHCD and ICRF heating experiments in H-mode plasmas on EAST

X.J. Zhang[1], Y.P. Zhao[1], B.N. Wan[1], B.J. Ding[1], G.S. Xu[1], X.Z. Gong[1], J.G. Li[1], Y. Lin[2], G. Taylor[3], J.M. Noterdaeme[4, 5], F. Braun[4], S. Wukitch[2], R. Magne[6], X. Litaudon[6], R. Kumazawa[7], H. Kasahara[7] and EAST Team

[1]*Institute of Plasma Physics, Chinese Academy of Sciences, Hefei 230031, China*
[2]*MIT Plasma Science and Fusion Center, Cambridge, MA 02139, USA*
[3]*Princeton Plasma Physics Laboratory, USA*
[4]*Max-Planck Institute for Plasma Physics, D-85748, Garching, Germany*
[5]*University of Gent, Belgium*
[6]*CEA, IRFM, F-13108 Saint-Paul Lez Durance, France*
[7]*National Institute for Fusion Science, Toki, Japan*

Abstract. An ICRF system with power up to 6.0 MW and a LHCD system up to 4MW have been applied for heating and current drive experiments on EAST. Intensive lithium wall coating was intensively used to reduce particle recycling and Hydrogen concentration in Deuterium plasma, which is needed for effective ICRF and LHCD power absorption in high density plasmas. Significant progress has been made with ICRF heating and LHW current drive for realizing the H-mode plasma operation in EAST. In 2010, H-mode was generated and sustained by LHCD alone, where lithium coating and gas puffing launcher mouth were applied to improve the LHCD power coupling and penetration into the core plasmas at high density of H-modes. During the last two experimental campaigns, ICRF Heating experiments were carried out at the fixed frequency of 27MHz, achieving effective ions and electrons heating with the H Minority Heating (H-MH) mode, where electrons are predominantly heated by collisions with high energy minority ions. The H-MH mode gave the best plasma performance, and realized H-mode alone in 2012. Combination of ICRF and LHW power injection generated the H-mode plasmas with various ELMy characteristics. The first successful application of the ICRF Heating in the D (He3) plasma was also achieved. The progress on ICRF heating, LHCD experiments and their application in achieving H-mode operation from last two years will be discussed in this report.

Keywords: LHCD, ICRH, H-Mode, EAST
PACS: R52.55.Fa, 52.50.Sw
Email: bnwan@ipp.ac.cn

INTRODUCTION

Experimental Advanced Superconducting Tokomak (EAST) is a full superconducting device with an advanced configuration in the world [1-4]. EAST has a major radius R = 1.85m and a minor radius a=0.48 m, with an elongation of 1.2–2 for Single-Null (SN) and Double Null (DN) divertor operations. Its purpose is to establish the scientific and technological basis for the next generation of tokamak reactors [5]. At initial operation phase, 2.0MW at 2.45GHz [6-7] and 1.5MW ICRH system [8-9] were equipped and recently upgraded to 4.0MW and 6.0MW respectively. With enhanced heating and current-drive capacities, EAST has achieved reproducible stationary H-mode plasmas of over 30 s and long-pulse diverted plasmas over 410 s in the 2012 experimental campaign.

By the baking of plasma-facing components and extensive Li wall conditioning, effective ICRF heating [10] was successfully performed in EAST during 2010 autumn campaign [11-12]. In the 2012 experimental campaign, ICRF heating is more effective with further reduced hydrogen concentration to 3%. The H Minority Heating mode gave the best plasma performance with improved lithium coating and much more effective ICRF heating, and realized H-mode alone [13]. The first effective ICRF heating was demonstrated with helium-3 as minority particles in the deuterium target plasma in EAST.

LHW coupling improvement by optimizing the outer gap and local gas puffing near the LHW launcher are necessary to reduce reflection and achieve reproducible stationary H-mode. Lower hybrid current drive (LHCD) [14–15] plays a key role in controlling current profile in tokamak experiments aimed at achieving important goals relevant to fusion plasma. Good lower hybrid wave (LHW)-plasma coupling is the first necessary condition for LHCD experiment and high current drive (CD) efficiency is important for driving plasma current and controlling

Radiofrequency Power in Plasmas
AIP Conf. Proc. 1580, 49-56 (2014); doi: 10.1063/1.4864501

current profile, especially for sustaining long pulse high confinement (H-mode). Aimed at H-mode plasma in EAST, LHW-plasma coupling and current drive experiments were continued after the 2010 campaign, especially, local gas puffing from electron (GIM_e) and ion side (GIM_i) of LHW antenna and high density experiments with LHCD.

In 2010 autumn campaign, EAST has achieved first H-mode plasma typically with type-III edge localized modes at an H factor of H89(y, 2) ~0.8 with about 1.0MW LHW power [16]. With a combination of ICRH and LHCD under a low recycling wall condition, a new type of stationary H mode discharges could be sustained longer than several ten times the energy confinement time. H-mode can only be accessed by ICRF heating in the LHW driven L-mode plasmas due to lower power absorption. In 2012 spring campaign, EAST has been well progressed. New features of H-mode plasmas have been reliably generated by combination of LHCD and ICRF power. Furthermore, the H-mode duration has been extended from 6.4 s in 2010 to over 30 s in 2012, achieving the world's longest H-mode plasma in a small-ELM regime with duration up to 32 s, much longer than several tens of the current diffusion time, with combined LHCD and ICRH, as shown in Fig. 1.

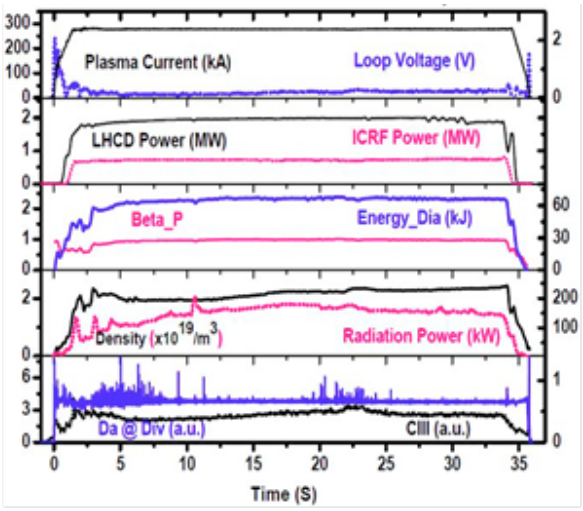

FIGURE 1. Long-pulse H-mode over 32 s achieved in EAST 2012 campaign with combined LHCD and ICRH.

ICRF HEATING EXPERIMENTS

The performance of ICRF heating has progressed steadily in the EAST. This is mainly because lithium wall conditioning was routinely used to reduce both impurity and hydrogen recycling and to improve the ICRF power absorption. In 2012 spring campaign, EAST capabilities have greatly been augmented. Graphite tiles on the low heat load area were replaced by molybdenum, except for the divertor regions. This modification allow to reduce Hydrogen concentration significantly from previous ~10% to ~3% in deuterium plasma after intensive Li wall coating, which allow more effective ICRF heating in minority heating scheme.

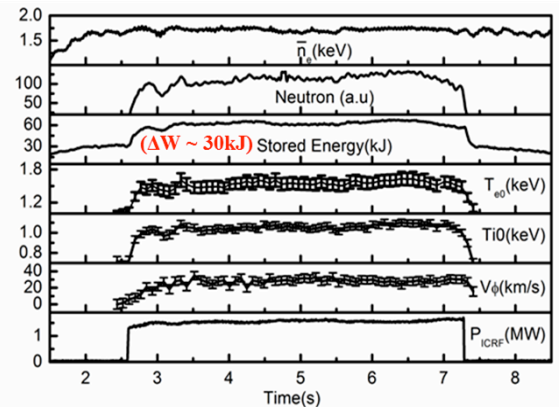

FIGURE 2. An example of typical ICRF Heating plasma discharge in EAST with 1.7MW of ICRF power injected from the B- and I- port antennas show effective electron and ions heating.

Both ions and electrons heating were observed in the H-minority heating scheme in a deuterium majority plasma. An example of ICRF heated discharge at Bt=1.96T and Ip=500kA and hydrogen concentration is about 3% is shown in Fig.2 where the B and I port antennas are operated in (0,pi) phasing and 27MHz. The neutron rate and stored energy are increased when ICRF switched on. A significant rise of central ions and electrons temperature measured by X-ray crystal spectrometer are seen. The sawtooth stabilization is also obtained during the ICRF pulse. This could be illustrated that the high-energy populations of H produced by MH is contributed to the sawtooth stabilization.

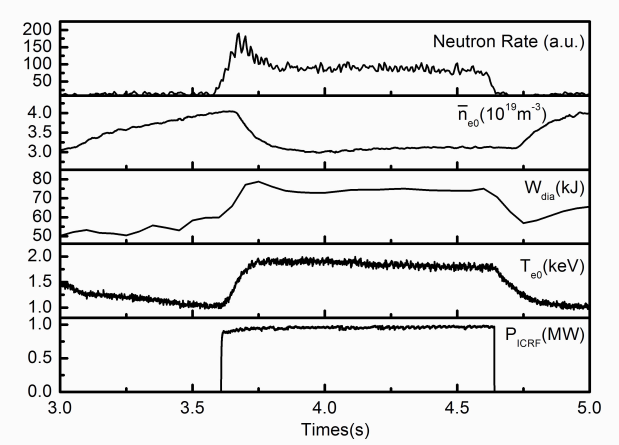

FIGURE 3. An example of ICRF Heating in EAST from an earlier campaign with 1.0 MW ICRF power at 27MHz injected from the O- and I- port antennas.

The second example of H Minority Heating from an earlier campaign is shown in Fig.3 where 1.0MW of ICRF power at 27MHz was injected from O and I port two strap antennas into a discharge at 2.0T and 500kA and hydrogen concentration is about 7%. One can clearly see that electron density drops by about 20% after the ICRF power is applied. Heating by ICRF waves may affect the underlying transport of particles in tokamak plasmas. Enhanced transport of particles may thus lead to reduced electron density. The increase in the electron temperature was above 1.0 keV. The stored energy has an increase of 30kJ.

With H Minority Heating mode in D(H) plasma, for the first time, the ICRF heated H mode has been reproducibly achieved with injected RF power of ~1.7MW launched by B- and I- port antennas. The H-mode plasma is sustained up to 3.45 s, as shown in Fig.4. H-modes started with a short ELM-free period, lasting ~ 500 ms, followed by type III ELMs (figure 4 (a)) with frequencies from 200Hz to 500Hz (figure4 (b)). Confinement times for the H-mode discharges are in the range of 110ms to 150ms for 1.7 MW of total heating power at 500 kA. The H factor, $H_{98IPB\,(y,\,2)}$, for the L mode plasma just before the transitions is about 0.5 and then up to 0.7±0.1.

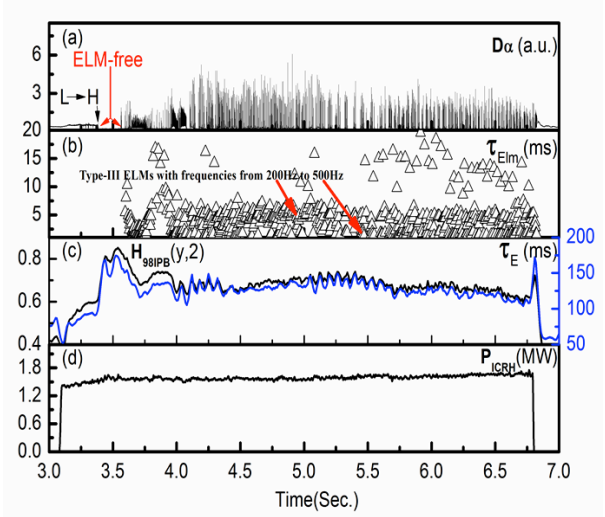

FIGURE 4. An example of ICRF heated H mode from the 2012 campaign with 1.7MW of ICRF power injected from the B- and I- port antennas.

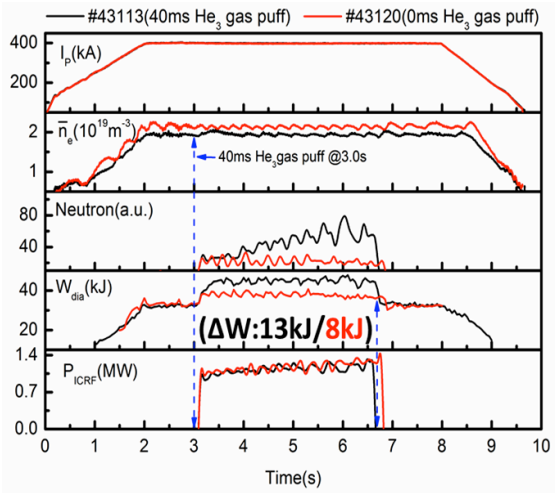

FIGURE 5. An example of ICRF Heating in D (He3) plasma from the 2012 campaign with 1.0MW of ICRF power injected from the B- and I- port antennas.

The first effective heating in D (^{3}He) plasma was observed. This is confirmed by the stored energy and neutron measurements. An example is shown in Fig.5. Traces of two discharges at different Helium 3 gas puff time are compared, where Bt=3.0T and Ip=400kA and hydrogen concentration is about 5%. The fusion neutron rate on both plasma decreases immediately after ICRF power is turned off. Greatly different neutron rates and the stored energy have been observed. This observations show that single pass absorption is weak for the discharge without Helium 3 gas puff. This is also confirmed by a big difference in the stored energy in these two shots.

EXPERIMENTS ON LHCD

LHW-plasma coupling depends strongly on the density at the grill mouth and, especially in H-mode, the density in front of the antenna decreases due to the large density gradient. Plasma-wave coupling deteriorates as the transition of L-H occurs, due to the steep gradient density profile in H-mode, which lowers the density at the grill mouth. The density is then recovered slowly until the H-L transition occurs. The plasma radiation has a correspondingly periodic characteristic behaviour during L-H and H-L transition. Such changes of radiated power and coupled LHW power may lead to the multiple L-H-L transitions, suggesting that the net power for H-mode plasma is marginal. Therefore, it is necessary to reduce impurity radiation and improve LHW-plasma coupling to sustain H-mode plasma, eg., by means of lithium coating and local gas puffing.

In order to improve LHW-plasma coupling, two gas pipes covering the total grill in the poloidal direction are installed near the LHW antenna in EAST. One is in the electron side (GIM_e), and the other is in the ion side (GIM_i). The totroidal angle between antenna and pipe is about 33 degree. The major radius of the pipe location is about 2400mm.Experiments of gas puffing from electron-side and ion-side on LHW-plasma are first performed in EAST. The plasma and LHW parameters are Ip = 400kA, Bt= 2T, and the launched spectrum of N//peak=2.1. It is performed with varying gas flow rate by investigating reflection coefficients and density measured by reciprocating probes. The electron density at the last closed flux surface (LCFS) and the RCs with different gas flow rate are plotted in Fig. 6(a) and (b). It is shown that the density is higher and the RC is lower in the case of gas puffing from GIM_e, meaning that it is more efficient to improve density with GIM_e puffing. Further comparison (see Fig. 7) shows that for a same density at the LCFS, the RC in the case of GIM_e puffing is a little smaller than that in the case of GIM_i puffing, implying a higher density at the grill mouth when gas puffing from electron-side. This can be explained the different movement direction of the electron after ionization. Usually, the gas is ionized by plasma potential and local LHW electric, etc. When puffing from GIM_e, the ionized electron moves toward to LHW antenna, whereas the one moves away from antenna when puffing from GIM_i. The electron moving to antenna will be useful to increase the grill density compared to the opposite direction, since the later is not magnetically connected to the grill due to some first components (e.g., limiter). Therefore, the density at the grill will be different even if with a same density at the LCFS, hence, leading to different RC. Such difference should depend on edge plasma parameter (e.g., temperature), which will be studied later. Above results suggest that gas puffing from electron-side is more efficient to improve LHW-plasma coupling.

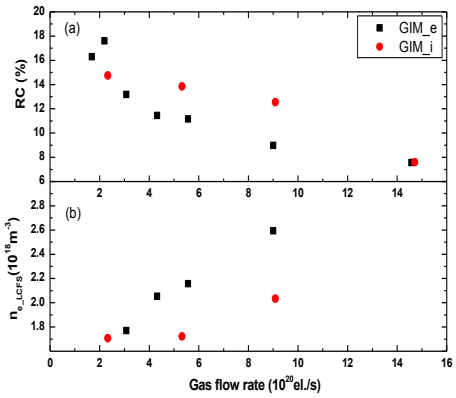

FIGURE 6. RC and ne_LCFS vs gas flow rate.

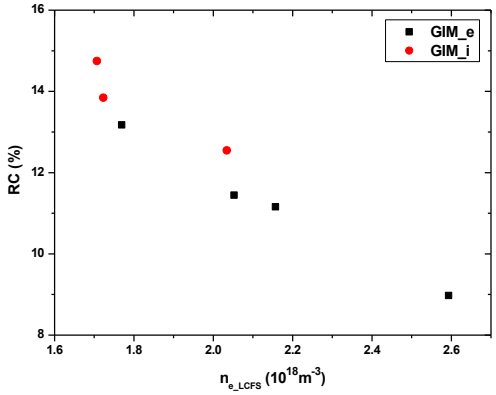

FIGURE 7. RC vs ne_LCFS.

High density is a challenge of LHCD experiments in H-mode discharges. In order to improve CD efficiency at high density, experiments were performed by increasing density in one discharge with different operation conditions, i.e., poor and strong lithiation, density feedback with gas puffing and supersonic molecular beam injection (SMBI). For comparison, the launched LHW spectrum is N//peak =2.1, the configuration is fixed double configuration, and local gas puffing from GIM_e is utilized in the experiments. Since the non-inductively driven plasma current is generally modest in high-density experiments, the LH effects can only be detected via the radiation generated by LH accelerated electrons. Therefore, the effect of driven current is estimated by the count of hard X-ray rate (20keV~200keV) normalized by the injected LHW power, which is proportional to current driven efficiency. The relationship between normalized bremsstrahlung emission and line averaged density (ne) is shown in Fig.8, indicating that with strong lithiation, the effect of current drive is much better than that poor one in the case of gas puffing. It is seen that in the strong lithized discharge, there is no sudden decrease of driven current, which deviates from the curve of 1/ne, until density up to $3.0\times10^{19}m^{-3}$, which is much larger the value of $2.0\times10^{19}m^{-3}$ in the poor lithiation. This is consistent with the previous studies that lithium coating is beneficial to increase CD efficiency at high density, due to the low cycling and high temperature in the lithium condition. It is also seen that for a similar lithiation, the current drive effect with SMBI is worse than that with gas puffing. The reason for this is not clear. The possible reason for this is the SDF due to the larger density fluctuation with the SMBI experiments in the edge region (Fig. 9. In addition, in the SMBI case, a relative high neutral deuterium radiation is observed. This may result in high density in the edge (Fig.10), leading to the low CD effect possibly due to PDI or CA.

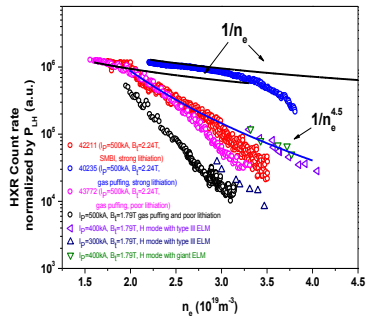

FIGURE 8. HXR vs density.

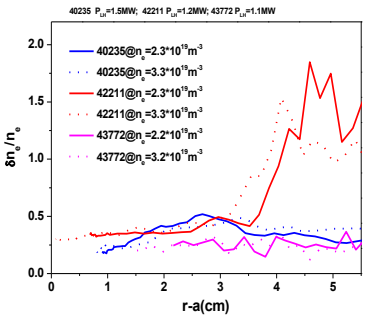

FIGURE 9. Density fluctuation in SOL.

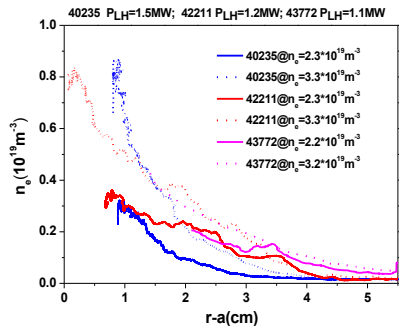

FIGURE 10. Density profile in SOL.

Wave accessibility and PDI have been suggested as possible explanations for the density limits observed on previous LHCD experiments. PDI is a three wave coupling process by which an incident lower hybrid wave at a frequency ω=ω0 decays into a low frequency branch, at ω=ω1~ωci<<ω0 and a daughter LH wave, at ω=ω0−ω1. The wavenumber of the daughter LH wave may upshift substantially, thereby reducing the current drive efficiency. Since the same magnetic toroidal field and the LHW spectrum are fixed in the experiments, the discrepancy in sharp decay of bremsstrahlung emission is not due to wave accessibility. In addition, the dependences of CD effect on

density are nearly consistent with the frequency of ion-cyclotron (IC) sideband (Fig.11), measured by a RF loop antenna located outside the machine, implying the sharp decay of HXR counts is correlated with PDI.

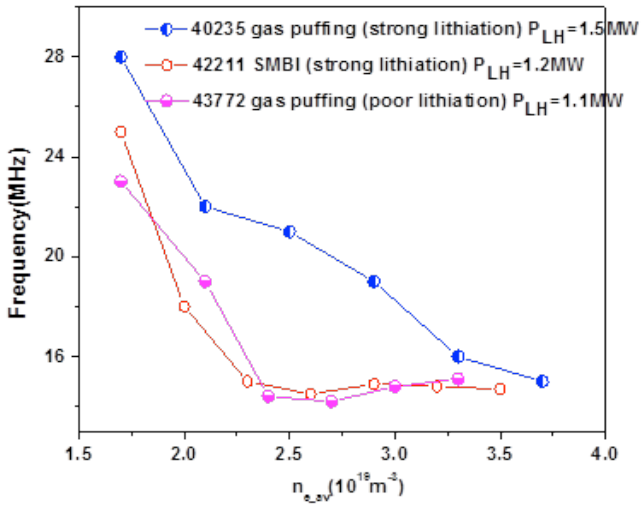

FIGURE 11. Frequency of IC sidebands.

Comparing the experimental data for different current and magnetic field, experiments also show that CD effect is better in higher plasma current or higher toroidal magnetic field, being in agreement with studies in Tore-Supra. This is because high plasma current is favorable to increase temperature, hence improving CD efficiency. The effect of magnetic field on efficiency is mainly ascribed to wave accessibility condition. By further comparing the counts in L- and H-mode, it is seen that CD efficiency in H-mode is larger than that in L-mode for a same density. This means that efficiency at high density could be improved in H-mode plasma.

APPLICATION OF LHCD AND ICRF HEATING IN THE EXPERIMENTS ON H MODE OPERATION

By increasing ICRF heating power in LHW driven plasmas, stationary ELMy H-mode with mixed type-I and small ELMs was achieved in EAST, as shown in FIG. 12. This H-mode regime is obtained at low density (ne/nG~0.46) by applying 1.2MW LHCD and 1.6MW ICRF in LSN configuration with bottom triangularity δ ~ 0.48. The H-mode operation appears to be more stable with LSN configuration. It could be because the strong particle control provided by the internal cryogenic pump beneath the out lower divertor plate.

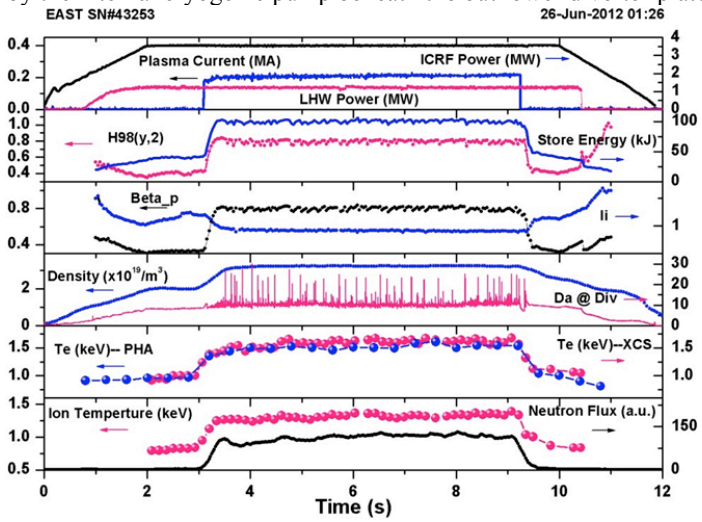

FIGURE 12. Stationary H-mode with mixed type-I and small ELMs.

By reducing plasma density at Ip~0.3MA and increasing ICRF heating power, type-I ELMy dominated H modewith good confinement, i.e. H98,y2~1,was achieved. Fig.13 shows such a typical H-mode discharge withthe central-line-averaged density at ne/nG~0.4 during the H-mode period. A profound loss of plasma-stored energy up to~10% was observed to be induced by the type-I ELMs.

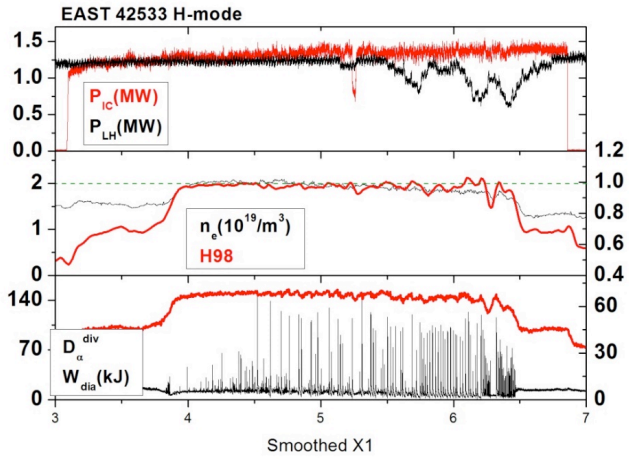

FIGURE 13. type-I ELMy H mode with H98,y2~1.

By increasing the density to ne/nG~0.62, an enhanced Da H-mode regime was obtained with LSN configuration and bottom triangularity δ ~ 0.43, which is characterized by two coherent mode[17] at the plasma edge with frequency ~ 30 kHz and ~200 kHz, enhanced Da emission and small ELMs, as shown in Fig. 14.

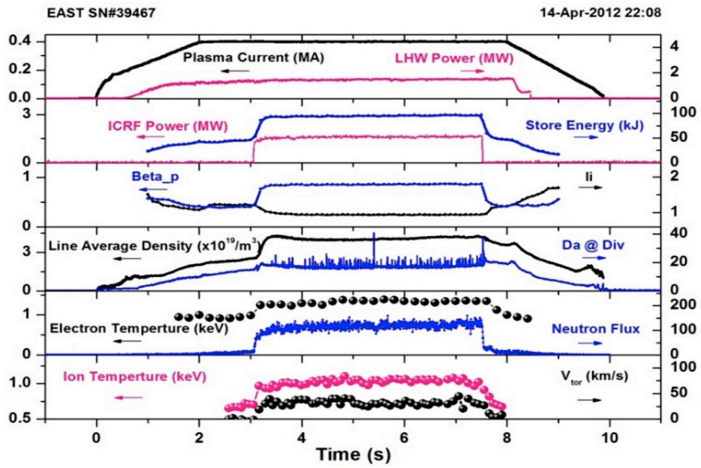

FIGURE 14. H mode with an Enhanced Da emission, irregular ELMs.

SUMMARY AND NEAR FUTURE PLAN

In summary, significant progress has been made on EAST toward long-pulse high-performance operation. EAST is now undertaking a new, extensive upgrade for high-power operation with a longer pulse. Figure 15 shows the distribution of auxiliary heating systems on EAST. EAST will be equipped with over 30 MW CW H&CD power and ITER-like W mono-block divertor, which will certainly produce more exciting results. These new capabilities will make EAST a unique facility to address some critical issues related to steady-state H-mode physics in RF dominated regimes for long-pulse operations under ITER relevant conditions in the near future, which will certainly produce more exciting results.

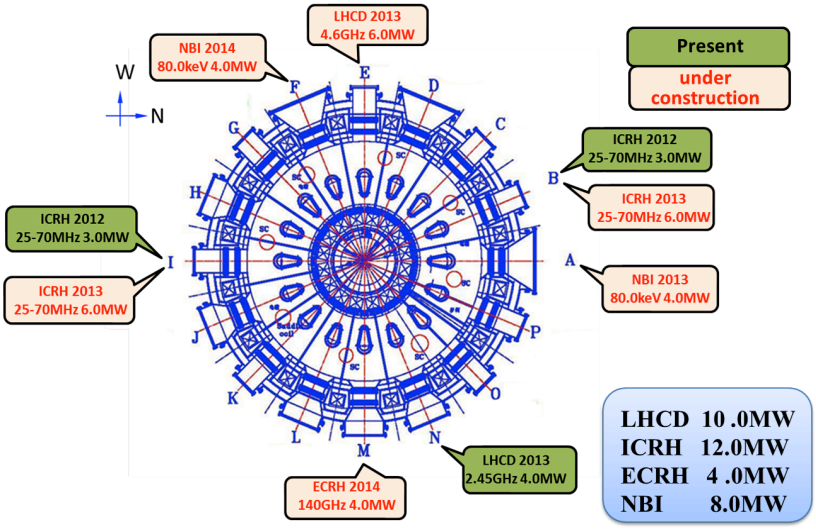

FIGURE 15. The distribution of auxiliary heating systems on EAST.

ACKNOWLEDGMENTS

The authors would like to acknowledge the support of and EAST operation and diagnostics group. This work was supported partially by the National Natural Science Foundation of China under Grant Nos. 11105179，10725523, 10721505, 10990210, 10990212, 11075182 and sponsored in part by National Magnetic Confinement Fusion Science Program of China under Contract 2011GB101000, 2011GB107000, 2011GB107001 and by JSPS-NRF-NSFC A3 Foresight Program in the field of Plasma Physics (NSFC no. 11261140328).

REFERENCES

1. Yuanxi Wan, et al, “Overview progress and future plan of EAST Project” Fusion energy 2006, Proc. Of 21th Int. Conf. (Chengdu, China 2006) (Vienna : IAEA) OV/1-1, http://www-naweb.iaea.org/napc/physics/fec/fec2006/dataset/index.html
2. Wan B.N. et al 2008 Proc. 22nd IAEA Conf. on Fusion Energy (Geneva, Switzerland, 2008), http://www-naweb.iaea.org/napc/physics/FEC/FEC2008/papers/ov 3-4.pdf
3. Wan B.N. et al 2010 Fusion Eng. Des. 85 1048
4. Wan B.N. and International Collaborators 2009 Nucl. Fusion 49 104011
5. Wan Y.X. et al 2000 Nucl. Fusion 40 1057
6. Zhao L. M., et al 2010 Plasma Sci. Tec. 12 118.
7. B. J. Ding, Y. L. Qin, W. K. Li, et al 2011 Phys. Plasma 18 082510.
8. Jiangang Li et al., Nucl. Fusion 51 (2011) 094007.
9. X.J.Zhang et al 2010 Proc. 23rd Int. Conf. on Fusion Energy (Daejeon, Republic of Korea, 2010) (Vienna: IAEA) http://www-pub.iaea.org/mtcd/meetings/PDFplus/2010/cn180/cn180 papers/exw p7-30.pdf
10. Zuo G.Z. et al., 2012 Plasma Phys. Control. Fusion 54 015014.
11. X.J. Zhang et al., Plasma Sci. Technol. 13(2011) 172
12. X.J.Zhang,et al., Nucl. Fusion 52 (2012) 032002.
13. X.J.Zhang,et al., Nucl. Fusion 53 (2013) 023004
14. Fisch N.J. 1978 Phys. Rev. Lett. 41 873.
15. Bernabei S. et al 1982 Phys. Rev. Lett. 49 1255.
16. G.S.Xu,et al., Nucl. Fusion 51 (2011) 125001B.
17. Wan et al., Proc. 24th Int. Conf. on Fusion Energy, San Diego, CA, 2012, OV/2-5.